

Short Note

Wave-equation migration from topography: Imaging Husky

Jeff Shragge¹

INTRODUCTION

Imaging land seismic data is wrought with many technical challenges that arise during different stages of seismic investigation: acquisition (e.g. irregular geometry), preprocessing (e.g. ground-roll suppression, statics), velocity estimation (e.g. near-surface complexity) and migration (e.g. rugged topography, uncertain velocities). Each of these complicating factors needs addressing before satisfactory final images are generated. Given the completion of each pre-migration processing step, one may choose from a variety of migration techniques; however, velocity profiles and geologic structures often are sufficiently complex to warrant wave-equation imaging. A caveat, though, is that wave-equation migration (WEM) is usually implemented with regularly sampled data on Cartesian meshes. Hence, conventional WEM from topography usually requires data regularization prior to migration.

Topographic data regularization approaches often include pre-migration datuming using statics corrections. These basic processes use vertical time-shifting of the wavefield to estimate the data recorded on a flat datum above or below the true acquisition surface. Standard migration techniques (e.g. wave-equation or Kirchhoff) may then be applied directly to the regularized dataset. However, the vertical wavefield propagation assumption usually is not satisfied in areas characterized by fast near-surface velocities and strong velocity gradients (e.g. in the Canadian Rocky Mountain Foothills) due to limited accuracy at propagation angles that deviate significantly from vertical. Hence, more advanced techniques able to incorporate topography are needed. A short and not exhaustive list of such methods (e.g. using more kinematically correct Kirchhoff operators (Bevc, 1997)) is presented in Shragge and Sava (2004).

In general, most wave-equation processing solutions to topographic data irregularity use a strategy of forcing data to conform to Cartesian geometry. The converse of this situation is to tailor wave-equation migration implementation to coordinate system meshes defined by the acquisition geometry. Shragge and Sava (2004), following the latter strategy, extend wave-equation migration to “topographic coordinate systems” conformal to acquisition topography. Although Shragge and Sava (2004) applied this approach to synthetic 2D data, they neither tested the algorithm on field data nor compared it to more conventional imaging from standard topography approaches (e.g. Kirchhoff migration). This paper addresses these issues

¹email: jeff@sep.stanford.edu

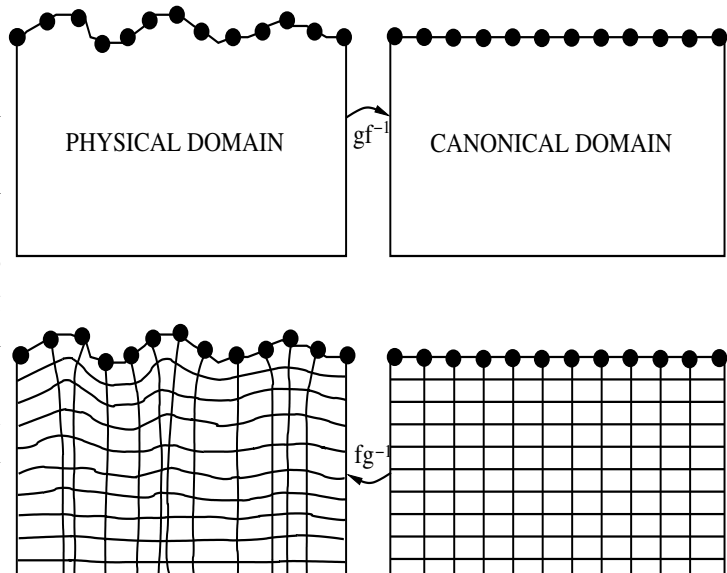
with imaging experiments using the Husky 2D land dataset acquired in the Canadian Rocky Mountain Foothills.

NON-TECHNICAL TECHNIQUE OVERVIEW

This section briefly describes the wave-equation migration from topography (TopoWEM) approach presented in Shragge and Sava (2004). Two theoretical developments are central to the technique: i) generating an orthogonal grid conformal with the acquisition surface using a conformal mapping approach; and ii) adapting wave-propagation physics to be consistent with the geometry of the computational mesh using Riemannian wavefield extrapolation (RWE) (Sava and Fomel, 2005). Conformal mapping transforms can be manipulated to generate an orthogonal coordinate system by computing a mapping from a topographically influenced domain to a rectangular mesh (c.f. Figure 1). First, the image of the boundary points in the physical domain (upper left) is found in the canonical domain (upper right) through composite mapping $g \cdot f^{-1}$ (where g and f^{-1} represent mappings from the physical domain to the unit circle and from the unit circle to a rectangle, respectively). A uniform mesh, specified in the canonical domain (lower right), is then mapped to the physical domain (bottom left) using the inverse relation $g^{-1} \cdot f$, creating an orthogonal mesh conformal to the topographic surface.

Figure 1: Cartoon showing the conformal mapping transform between topographic and rectangular domains. Top left: topographic domain with data acquisition points; Top right: domain boundary in top left mapped to a rectangular domain under mapping $g \cdot f^{-1}$; Bottom right: uniform grid in canonical domain; and bottom left: (locally) orthogonal grid in physical domain generated by mapping grid in bottom right under relation $g^{-1} \cdot f$.

`jeff1-map1` [NR]



The second step is to specify the RWE extrapolation equations appropriate for the generated topographic coordinate system. This approach specifies a wave-equation dispersion appropriate for one-way wavefield extrapolation in generalized coordinate systems. Shragge and Sava (2004) discusses how to perform wave-equation migration directly from topographic coordinate systems, and illustrates this approach with a synthetic 2D data example.

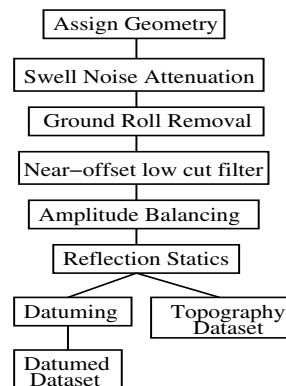
HUSKY 2D LAND DATASET

The Husky 2D land spec dataset was acquired by Husky Oil and Talisman Energy in a complex fold and thrust belt of the Canadian Rocky Mountain Foothills. This dataset, released by Husky Oil to aid industry technological development, was the focus of a processing workshop at the SEG's 1995 Annual General Meeting. The dataset consists of 143 shot-records, with a nominal source and receiver spacing of 100 m and 20 m, respectively. Shot-records contain approximately 300 channels per shot in a split-spread geometry with a maximum offset of ± 4000 m. Overall, this high-quality field dataset exhibits many typical data attributes: realistic near-surface effects, elevation changes, and associated geologic information and ambiguity. In addition, the dataset is in a location of minimal 3D structure, which provides a good test for 2D imaging algorithms.

Preprocessing

Although the Husky dataset is of high quality, significant preprocessing is required to enhance signal quality. Data processing steps, applied using the proprietary OMEGA processing package, are listed in Figure 2. After geometry assignment, a swell-noise debursting algorithm was applied in the shot- and receiver-record and CMP domains to reduce anomalous low-frequency noise. Ground roll suppression and near-offset bandpass filtering subsequently reduced ground roll and airwave noise. Application of de-spiking and surface-consistent amplitude modules improved the relative amplitude balance across the shot-record and offset panels.

Figure 2: Husky data processing flow chart. jeff1-flow [NR]



Static time shifts were then compiled to generate a second datumed dataset. This dataset was generated by applying two static time shifts - one from the source/receiver location to an intermediate CMP datum, and a second to a constant elevation of -1800 m (assuming a 3200 m/s replacement velocity layer). Reflection statics (that optimized the power of the constant velocity scan stack) also were applied to both datasets. Figure 3 presents a comparison of a shot-record before and after data processing.

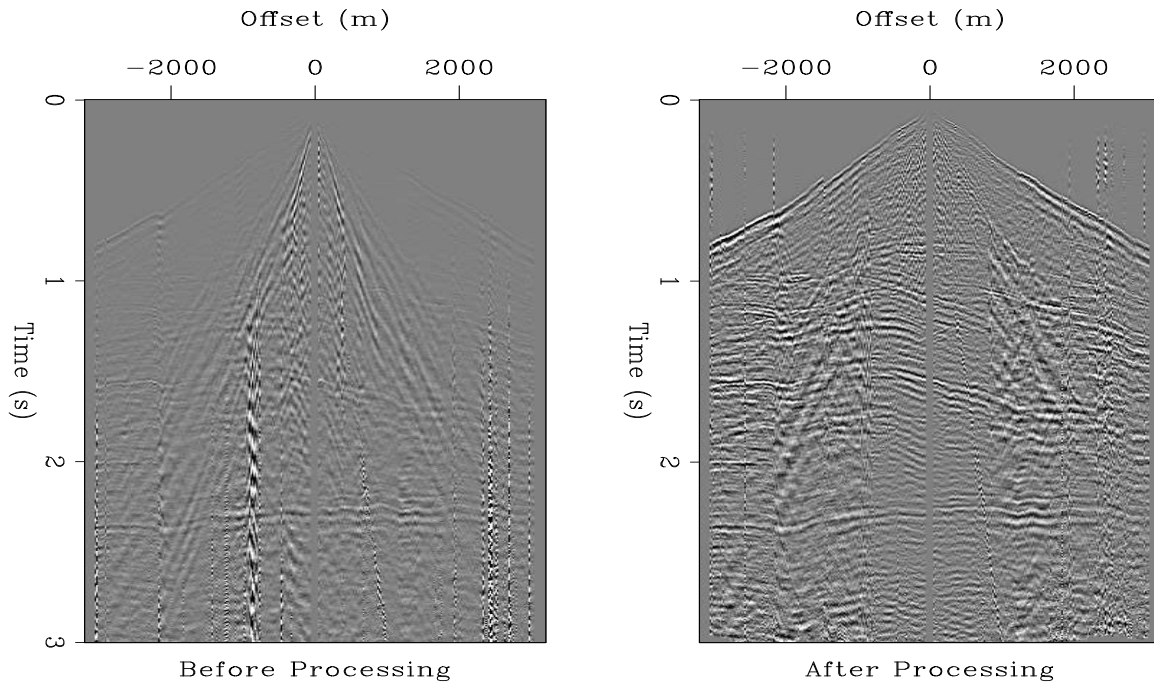


Figure 3: Sample Husky dataset shot-record before (left) and after (right) preprocessing. `jeff1-data_examp` [CR]

Migration Velocity Profile

Husky Oil also included a geologically derived velocity model in their deliverables. The near-surface component of this model is shown in top panel of figure 4. The model was developed from the combination of surface geologic observations, well-ties from 8-10 nearby wells and walk-away VSPs. Refraction tomography inversion of first-break arrival times (c.f. figure 3) provided a better estimate of the near-surface velocity profile (middle panel). The top 200 m of the refraction tomography model were grafted onto the geologic model, which was subsequently smoothed to create the migration velocity profile (bottom panel). The full migration velocity profile (figure 5) shows an intricate near-surface geologic environment characterized by complex faulting and folding and strong velocity contrast. Near-surface velocities are seismically fast with values ranging between 3600 m/s and 4800 m/s.

Imaging Results

Imaging tests were conducted on the topographic (WEM) and datumed (Kirchhoff migration) datasets. Figure 6 presents the results of imaging with the TopoWEM approach. Near-surface dipping reflectors are well-imaged, as are those above and at the basement. Note, though, that reflectors are somewhat broken up in some locations, especially in the basement. Angle gathers (not shown here) are generally flat; however, the presence of residual curvature indicates velocity model inaccuracy, and suggests that additional work to improve the currently

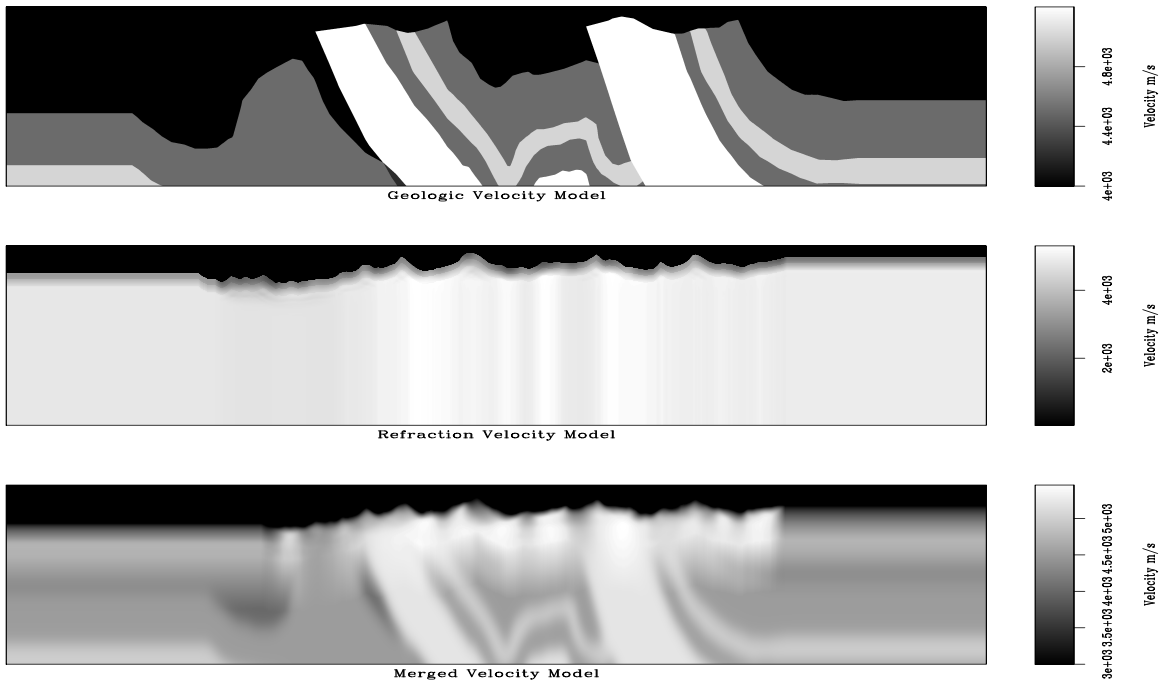


Figure 4: Initial velocity profile. Top: geologic velocity model; Middle: refraction to-mography velocity profile; and Bottom: merged geologic and refraction velocity profiles. `jeff1-vel_init` [CR]

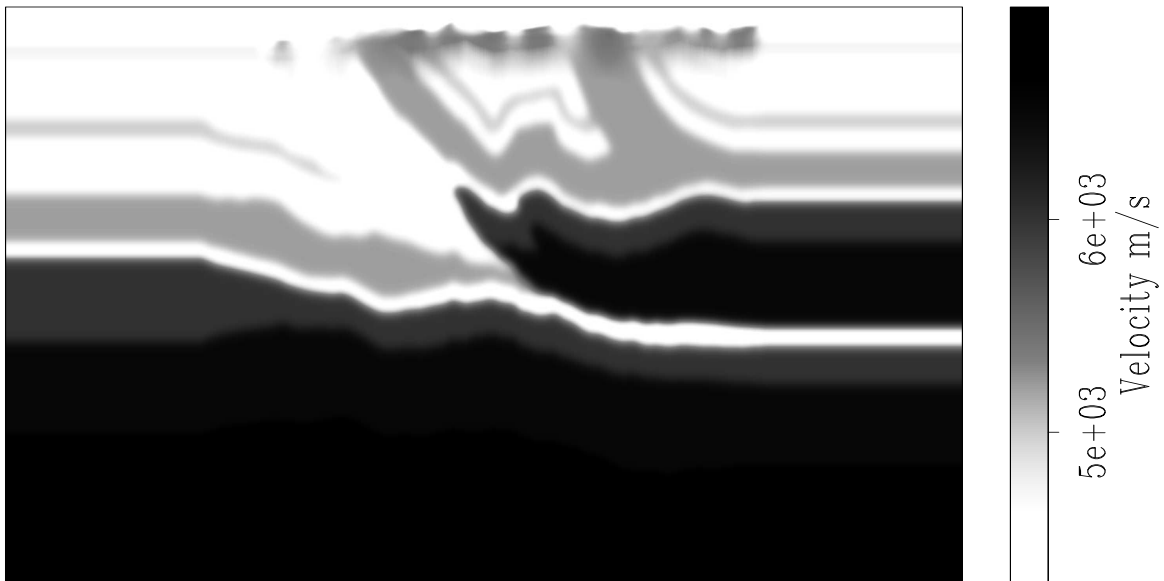
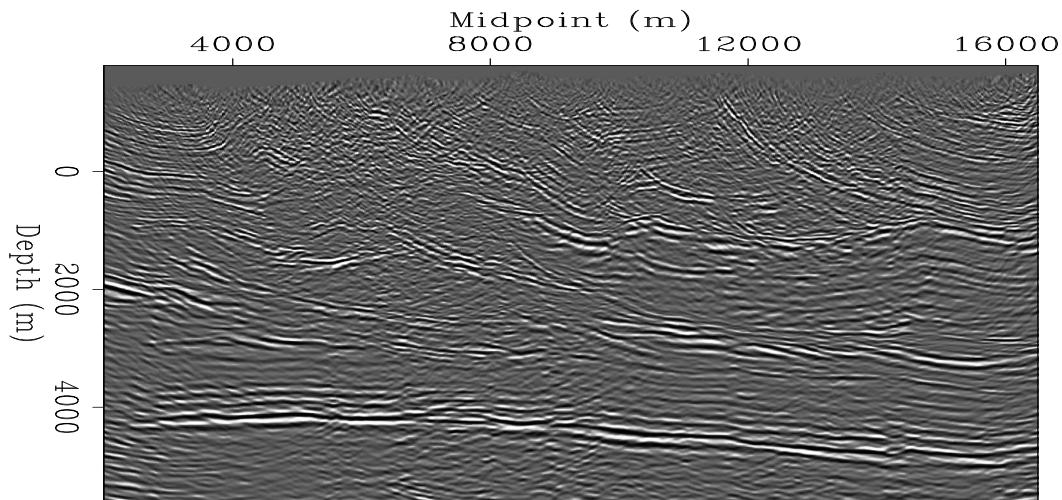


Figure 5: Migration velocity profile. `jeff1-vel_final` [CR]

geologically derived velocity model is warranted.



WEM from Topography – 3 Slow and 7 Geom. refs

Figure 6: Imaging results for wave-equation migration from topography. jeff1-TopoWEM1
[CR]

Figure 7 presents the results of migrating the datumed dataset using a Kirchhoff algorithm. Image quality is good at mid-to-basement depths; however, near-surface reflectors observed in the TopoWEM image are not visible. This could be due to additional internal velocity model smoothing in the proprietary Kirchhoff migration code, or to the failure of the vertical datuming approximation, which distorts wave-propagation paths and defocuses the near-surface image. (A Kirchhoff migration test from topography has not yet been conducted.)

CONCLUDING REMARKS

The Husky data migration test results indicate that the TopoWEM approach is a viable migration from topography technique. This approach produced images of near-surface structure superior to Kirchhoff migration from a flat datum. However, future tests will create a better benchmark by comparing these results to Kirchhoff migration from topography. Kirchhoff migration from a flat datum results were similar at mid-to-basement depths indicating that the major imaging advantage probably is localized to the near-surface. Subsurface gathers for images indicate, however, that further work is needed to improve the velocity model, which may lead to a more definitive statement about the relative merits of the TopoWEM approach.

ACKNOWLEDGMENTS

I would like to thank the Seismic Imaging team at ExxonMobil Upstream Research for providing a good environment that allowed me to conduct the work reported in this paper. A big

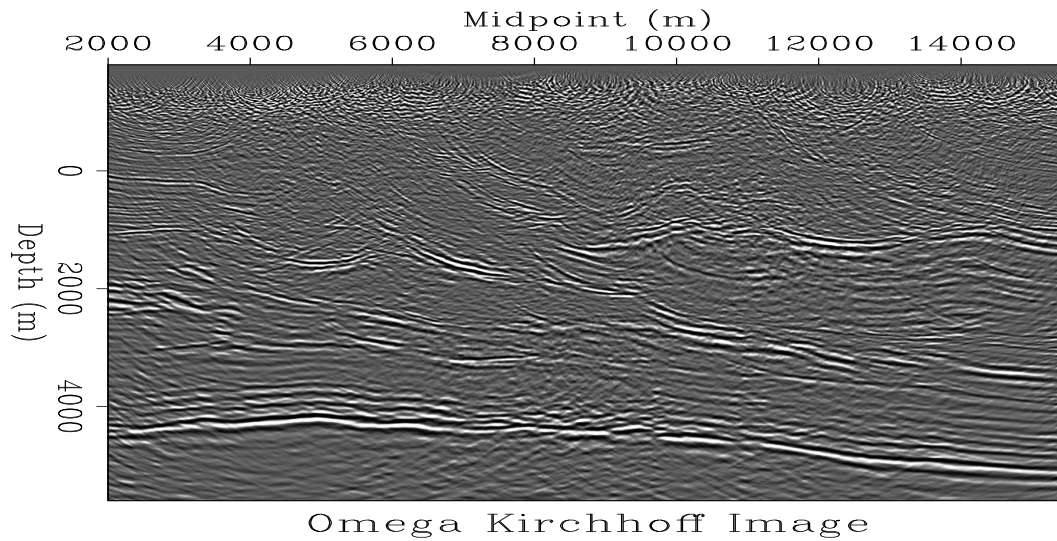


Figure 7: Imaging results for Kirchhoff migration of dataset from a flat datum. jeff1-Kirch
[CR]

thank-you to Tom Dickens for both excellent mentorship and his assistance with the data pre-processing. Husky Oil and Talisman Energy are acknowledged for releasing the Husky dataset used in these field test results.

REFERENCES

- Bevc, D., 1997, Flooding the topography: Wave-equation datuming of land data with rugged acquisition topography: *Geophysics*, **62**, 1558–1569.
- Sava, P., and Fomel, S., 2005, Riemannian wavefield extrapolation: *Geophysics*, pages T45–T56.
- Shragge, J., and Sava, P., 2004, Incorporating topography into wave-equation imaging through conformal mapping: *SEP-117*, 27–42.